

The role of oxidative stress on molybdenum enzymes and ischemic reperfusion injury in hyperuricaemic patients. An infrared spectroscopic study

Mamareli V¹, Tanis O¹, Anastassopoulou J^{2,3*}, Kyriakidou M², Mamareli CH², Kouli M¹, Theophanides T² and Mamarelis I⁴

¹National Technical University of Athens, Chemical Engineering School, Materials Science and Engineering, Zografou Campus, Athens, Greece

²National Technical University of Athens, Chemical Engineering School, Radiation Chemistry & Biospectroscopy, Zografou Campus, Athens, Greece

³International Institute of Anticancer Research, 1st km Kapandritiou-Kalamou Road, Kapandriti, Attiki, Greece

⁴Department of Cardiology, NIMTS Veterans Army Hospital of Athens, Greece

Abstract

There are many clinical evidences that hyperuricemia is a risk factor for the development of peripheral carotid and coronary vascular diseases. However, the mechanism of elevated uric acid concentration in biological systems is not yet clear. In the present work Fourier transform infrared (FT-IR) spectroscopy was used to evaluate the mechanism of calcification and plaque formation in carotid arteries in hyperuricaemic patients. Comparison between the spectra of carotid arteries from patients with elevated uric acid values and spectra obtained from patients with normal uric acid values showed structural changes of the characteristic spectral bands in the region 4000-500 cm⁻¹. These changes were related with changes in the concentration of the serum uric acid and the clinical history of the patients. The intensity decrease of the infrared bands in the region 1650-1500 cm⁻¹ was associated with the decrease of the apolipoprotein ratio, ApoI/ApoII, which corresponds to HDL (High Density Lipoproteins) and the regulation of the LDL (Low Density Lipoproteins), which are related to oxidation stress. The infrared band at 1467 cm⁻¹ indicated the presence of urea components as a result of the metabolic pathway. The shape and the intensity of the bands between 1250-900 cm⁻¹ depend on the glycation-end products of the diseases. SEM-EDX chemical analysis showed fibril formation and molybdenum release in hyperuricaemic patients.

Introduction

The term oxidative stress was introduced by B. Seis in 1985 in order to characterize the imbalance of endogenous antioxidants and free radical activity [1]. There are many papers on oxidative stress showing that it provokes inflammation, ischemia and cardiovascular diseases [2,3]. It is known that the oxidative stress affects the redox potential of the cells leading to damage of lipids, proteins, DNA, as well as the enzymes inducing fragmentations, peroxidation of the molecules, inhibiting thus the recovering of the damaged molecules. The free radicals are continuously produced endogenously in the living cells from metabolites, while external factors, such as cosmic rays, medical diagnostic techniques, and xenobiotics lead also to free radical production. Free radicals, because of the non-paired electron presence, are very reactive species and have the tendency to transfer or attract electrons in order to pair them and be stabilized. In all cases, it is necessary to have excess of electron transfer reactions, which activate the oxygen molecules as electron acceptors, and prevent the accumulation of damaged products which induce pathological effects. The active centre of the enzymes contains metal ions which could be excellent electron acceptors, as well as donors. Xanthine oxidoreductase (XOR) is a molybdenum-iron sulphur flavoprotein enzyme. Molybdenum is a transition metal and the possibility that it might have a biological function was recognized by Bortels in 1930, who reported that it acted as a catalyst in the fixation of nitrogen by *Arthrobacter chroococcum* [4] Molybdenum enzymes catalyse the oxidation of hypoxanthine to xanthine and the oxidation of xanthine to uric acid as final product. Xanthine is involved in purine and uric acid

(UA) catabolism and is implicated in the pathogenesis of hypertension [5]. It is believed that oxygen free radicals which are produced from XOR exert arrhythmogenic and cytotoxic effects in ischemic heart. Although uric acid has antioxidant properties [6], many recent studies suggest that it is an important risk factor for cardiovascular diseases [7-9]. However, its role at the molecular level is not yet well understood.

In order to study the mechanism of carotid atherogenesis at a molecular level we used Fourier Transform Infrared (FT-IR) spectroscopy. FT-IR spectroscopy is constantly gaining the attention of scientists in the study of biological molecules and diagnosis of diseases. FT-IR spectroscopy is a powerful, simple, fast and non-destructive method, which provides simultaneously information about all the components of the tissue at a molecular level. The individual spectral bands are the "fingerprint" not only of the chemical components of the tissues, such as proteins, phospholipids, DNA, but also of the disease [10-17]. By using FT-IR spectroscopy it is easy to elucidate structural features of proteins' secondary structure, such as protein folding, which could be used as "marker bands" for the diagnosis and the progression

*Correspondence to: Jane Anastassopoulou, International Institute of Anticancer Research, 1st km Kapandritiou-Kalamou Road, P.O. Box 22, Kapandriti, Attiki, Greece, Tel: (+30) 6073013308; E-mail: ianastas@central.ntua.gr

Key words: infrared spectroscopy, oxidative stress, molybdenum enzymes, hyperuricemia uric acid, SEM-EDEX

Received: October 31, 2019; **Accepted:** November 15, 2019; **Published:** November 18, 2019

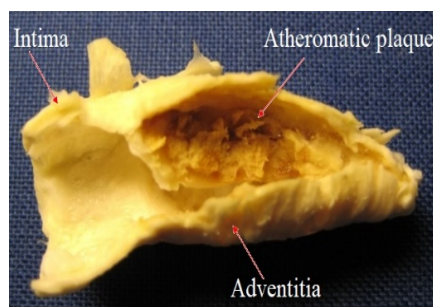
of the diseases [10-16]. Although a biological sample is complex, there are only a few main features that dominate the infrared spectrum, and it is essential to understand the origin of such absorption bands of the functional groups. In proteins the peptide bond (-NHCO-) gives rise to five strong characteristic bands, e.g. amide A and amide B, the amide I, due mostly to stretching frequency of $\nu\text{C}=\text{O}$, $\nu\text{C}-\text{N}$ and δNH frequencies, which mainly characterize the strength of the hydrogen bond between intermolecular and intramolecular interactions in the helices. The frequency of this amide I band is located in the 1650-1675 cm^{-1} spectral region showing the strength of the C=O frequency and its involvement in hydrogen bonding of the peptide bond in proteins [18]. The amide II band originates from the coupling of three frequencies of $\nu\text{C}-\text{N}$ stretching and in-plane bending of $\delta\text{N}-\text{H}$ of peptide bond -NHCO- and it absorbs and gives a characteristic band in the region of 1500-1575 cm^{-1} [19-21]. This amide II band is sensitive to conformational changes of proteins. The positions of the frequencies are energy profiles of the amide I and amide II bands. The amide III band originates from the coupling of $\nu\text{C}-\text{N}$ stretching vibration and $\delta\text{N}-\text{H}$ out-of-plane bending and is found as a medium or weak band in the region of 1200-1300 cm^{-1} . The amide A and amide B frequencies are found in the high energy region of stretching frequencies of $\nu\text{N}-\text{H}$ 3300-3200 cm^{-1} and are normally hydrogen bonded to C=O groups of -NHCO- in α -helix.

In lipids, the bands which arise from the stretching vibrations of methyl (νCH_3) and methylene (νCH_2) groups are found in the region 2800-3100 cm^{-1} . The bands related with $\nu\text{C}=\text{C}$ of unsaturated lipid chains are found near 1660 cm^{-1} and a weak band near 3080 cm^{-1} was assigned to the stretching frequency of olefinic $\nu=\text{C}-\text{H}$. The carboxylic stretching frequencies are characteristic and are found in the $\nu\text{O}-\text{H}$ region of the hydroxyl absorption band in the 3600-3500 cm^{-1} region, whereas the $\nu\text{C}=\text{O}$ carbonyl strong absorption band is found near 1740-1720 cm^{-1} [20,21]. Moreover, changes of the ratio between characteristic spectral bands gives even more information about the effect of the disease on the tissues [19,22].

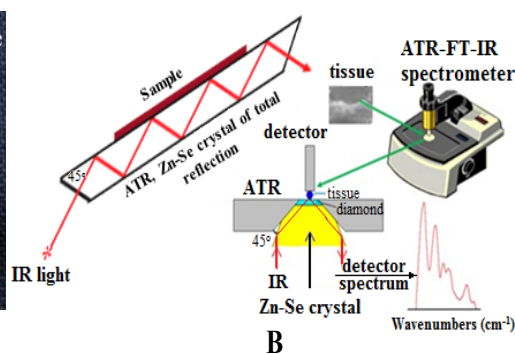
Materials and methods

Biopsies

For the present study, 150 biopsies of atheromatic plaques were used that were received from patients (age 53-84 years) who underwent carotid endarterectomy. All the patients were smokers and 30 of them were hyperuricaemic. After removal, the samples were immediately fixed in formalin solution.



A



B

Figure 1. A) Carotid atheroma. The arrows show the parts of the tissue which were analysed. B) Schematic presentation of ATR (attenuated total reflection) technique for recording FT-IR spectra. The infrared light passing through a Zn-Se crystal and after many reflections through the crystal and the sample on the surface, is collected by the detector. ATR allows us to record in different parts of the same sample.

FT-IR spectra

FT-IR spectra were recorded using Nicolet 6700 thermoscientific spectrometer (USA) with an attenuated total reflection (ATR) crystal. The biopsies were washed with hydrogen peroxide and high distilled water to remove the blood. In order to minimize the signal-to-noise ratio each spectrum consisted of 120 co-added spectra at a spectral resolution of 4 cm^{-1} . The OMINC 7.2a software was used to analyse the spectra. Each infrared spectrum was compared with the corresponding infrared spectra of all other patients, taking into account their clinical history.

With the ATR accessory technique, the biological samples were not homogenized. This allowed us to study different parts of the biopsies (Figure 1A) as it is shown with the arrows.

The samples were not fixed in paraffin, since it was found that valuable information on the disease was lost, because by removing the paraffin from the samples were removed also the soluble products in it produced during the disease. We have seen that using solvents such as hexane or DMSO the aggregates formed during the disease development preferred the lipophilic environment and they were not detected in the spectra [2].

Scanning Electron microscopy, SEM

The morphology of the surface of carotids was obtained by using the Scanning Electron Microscope (SEM) (from Fei Co, The Netherlands). This was coupled with energy dispersive X-ray (EDX) apparatus for elementary chemical analysis of different sites or spots of the carotids. The samples were not covered with carbon or gold in order to avoid the reaction of secondary electrons.

Ethics

The samples were taken after the removal of the patients, according to the Greek ethical rules and the permission of the Scientific Board of the 401 Army General Hospital.

Results and discussion

In Figure 2 are shown the representative spectra in the region 4,000-700 cm^{-1} of carotid atheromas obtained from (a) control healthy patient, (b) patient with normal serum uric acid and (c) hyperuricaemic patient.

Spectral region 4,000-3,000 cm^{-1}

Comparison between the spectra showed considerable intensity changes and frequency shifts in the entire spectral region. In the spectral region 4,000-3,000 cm^{-1} are found the bands that arise from

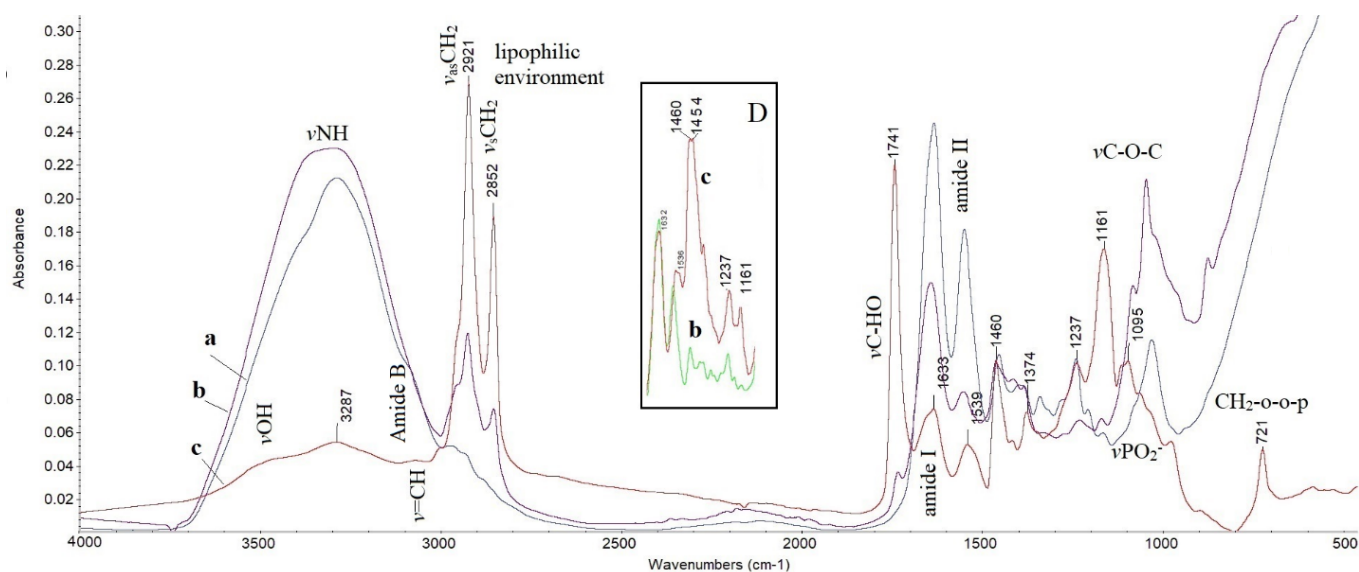


Figure 2. Representative FT-IR spectra of carotid atheroma. A) c healthy patient control sample, B) from patient with normal serum uric acid and C) from hyperuricaemic patient. D) Insert spectra with characteristic bands of hyperuricaemic patients.

the stretching vibrations of νOH of water and saccharide molecules and νNH groups of proteins in the cell [14,15,23,24].

In the spectra of hyperuricaemic patients the broad band at about $3,527\text{ cm}^{-1}$ on the higher side of the energy of the νOH vibration is assigned to the frequency of the weaker hydrogen bonded $-\text{OH}$ groups [25]. These hydroxyl groups reflect the hydroperoxidation of lipids, proteins and glycosides [21].

The next intense band at $3,287\text{ cm}^{-1}$ is assigned to stretching νNH vibrations of proteins in amide A conformation [22]. This band decreases strongly in the spectra of hyperuricaemic patients, leading to the result that the elevated uric acid affects the conformational structure of proteins. In the spectra of patients with normal serum uric acid this band becomes broader, suggesting that the atheromatic plaques of the patients contained a higher number of free $-\text{NH}_2$ groups.

The weak band at $3,080\text{ cm}^{-1}$ indicates that the proteins changed their conformation and are in the amide B configuration [18,25]. This means that the effect of the NH group of the peptide bond $-\text{NHCO}-$ is stronger than that of $\text{C}=\text{O}$, unlike amide A, where the effect of $\text{C}=\text{O}$ is stronger, suggesting different hydrogen bonds in length and strength that hold the protein strands together. We noticed that this band is very important for the characterization of the progression of the disease [3]. The band at $3,060\text{ cm}^{-1}$ is assigned to stretching vibrations of the terminal olefinic $\nu=\text{CH}$ mode, confirming the implication of oxidative stress during the disease development. This band's intensity was found to be proportional to LDL cholesterol concentration of the patients [2,23-24].

Spectral region $3,000\text{--}2,850\text{ cm}^{-1}$

The bands that appear in the region $3,000\text{--}2,850\text{ cm}^{-1}$ originate from the stretching vibrations of methyl ($-\text{CH}_3$) and methylene ($-\text{CH}_2$) groups, mostly from membrane lipids. The intensities of these bands are weak in the control spectra, but in the hyperuricaemic patients they become very strong. As it is shown, the stretching vibration bands of $\nu_{\text{as}}\text{CH}_3$ and $\nu_{\text{s}}\text{CH}_3$ groups at $2,958\text{ cm}^{-1}$ and $2,876\text{ cm}^{-1}$ respectively, have almost disappeared. On the contrary, the intensities of the absorption bands of $\nu_{\text{as}}\text{CH}_2$ and $\nu_{\text{s}}\text{CH}_2$ groups at $2,921\text{ cm}^{-1}$ and $2,852\text{ cm}^{-1}$ increase,

indicating changes of the flexibility and permeability of membranes, which upon the disease became more lipophilic and more ordered [2,23-24]. Deconvolution analysis of these bands shows a new band at $2,893\text{ cm}^{-1}$, which is assigned to the branched alkyl chain. Based on that, it is suggested that during the disease's progression, free hydroxyl radicals ($\text{HO}\cdot$) are produced through metabolic pathways and react with lipid chains leading to the formation of alkyl free radicals and then to radical-radical reactions in order to form stable products. The branched polymerization was also observed with SEM microscope.

Region $1,800\text{--}1,500\text{ cm}^{-1}$

This region is very important to study the changes which are induced from the diseases. The band at $1,741\text{ cm}^{-1}$ is attributed to aldehyde νCHO vibration mode. This band is a "marker band", which also shows the progression of the disease. As it is shown (Figure 2), the intensity of this band increases considerably in the spectra of hyperuricaemic patients and it is associated with lipid peroxidation of the biological membranes [2,23-24]. Our findings are in agreement with literature data, where it was observed in animal models during ischemia/reoxygenation [26]. A further increase of the intensity of the band at $1,741\text{ cm}^{-1}$ was observed in hyperuricaemic patients who were also diabetic.

The next intense band at $1,650\text{ cm}^{-1}$ is assigned to $\nu\text{C}=\text{O}$ of amide I of the peptide bond $-\text{NHCO}-$. This band decreases in intensity and shifts to lower wavenumber at $1,633\text{ cm}^{-1}$ depending on the increase of serum uric acid. Deconvolution analysis showed three bands at: $1,691\text{ cm}^{-1}$, $1,652\text{ cm}^{-1}$ and $1,625\text{ cm}^{-1}$ corresponding to antiparallel β -sheet, α -helix, random coil upon the disease development [23-25]. The β -sheet formation confirms the development of lipophilic environment, which is induced by the oxidation of membranes and amyloid like protein formation. The amide II band becomes broad and deconvolution analysis showed three bands at $1,550\text{ cm}^{-1}$, $1,540\text{ cm}^{-1}$ and $1,514\text{ cm}^{-1}$ upon amyloid protein formation. These bands are very characteristic and are observed in many diseases related to oxidative stress. After washing the biopsies in hexane, a non-polar solvent, it was found that the intensity decrease of the amide I and II bands was associated with the decrease of ApoI/ApoII ratio, which correspond to HDL and control LDL [27].

Spectral region 1,500-700 cm⁻¹

In this spectral region we get important information about the advanced glycation end products (AGEs) of the atheromatic plaques. Important bands are located at 1,460 cm⁻¹ and 1,454 cm⁻¹ as shown in the insert spectra D in figure 2. The first band derives from the asymmetric stretching vibration of $\nu_{as}NC$ bond of urea [28]. The intensity and shape of the first band is also related to other parameters, such as elevated serum glucose in patients. The second band at 1,454 cm⁻¹ is assigned to symmetric stretching vibration of $\nu_3CO_3^{2-}$ anions [29,30]. The latter band in combination with the observed band at 874 cm⁻¹, which is assigned to $\nu_4CO_3^{2-}$ vibrations suggest that the atheromatic plaque contains calcium carbonate salts and that acidosis could take place during the atheromatic plaque formation. These results are in accordance with literature data, where it was reported that under anaerobic conditions, low pH induces hydrolysis of ATP and affects the calcium homeostasis. It was described that during oxidative stress the Ca²⁺ cations enter in the cycle of CO₂ and yield calcium carbonates, which inactivate NADH and thus lead to cardiovascular diseases [31]. Moreover, accumulation of Ca²⁺ has been found to inactivate the protein folding messengers through the disulfide bond formation (-S-S-) and electron transfer reactions between thiol-disulfide bonds [32].

In the spectral region 1,300-900 cm⁻¹ the bands arise from amide III, the endo- and exo- stretching vibrations of $\nu-C-O-C-$ of sugars, $\nu C-O-P-O$ of sugar phosphate modes and νPO_2^- in phosphodiester groups of the phospholipids and DNA (Figure 2). This region could be characterized as the “fingerprint” of sugar molecules. In the spectra of the patients with elevated values of serum uric acid, an increase in

intensity of the bands at 1,237 and 1,161 cm⁻¹, which are assigned to sugars, was observed (Figure 2b and 2c). This is most likely due to glycation of collagen under oxidative conditions [33]. The changes were more pronounced in patients with elevated also the glucose in their serum. From the shape of the spectral band near 1095 cm⁻¹ it is suggested that the formation of calcium phosphate salts arise mostly from the reaction of calcium cations with the negative oxygen atoms of phospholipids.

SEM-EDX analysis

Figure 3 illustrates the architecture of the carotid artery of a hyperuricaemic patient. As it is shown, the morphology is not homogenous, but it contains foam cells, fibrils and inorganic salts in different sizes. The detection of fibrils is in accordance with the spectroscopic findings concerning the bands related to β -sheets which lead to amyloid protein formation. SEM-EDX chemical elementary analysis shows the presence of nitrogen (N), phosphorous (P), chloride (Cl), sodium (Na), magnesium (Mg), calcium (Ca) and molybdenum (Mo).

It must be noted that molybdenum was found in the carotid arteries as well as the aortic valve of hyperuricaemic patients only by performing SEM analysis. This observation indicates that in patients with excess serum uric acid the redox potential of molybdenum has been changed. In order to explain the presence of molybdenum in the atherosclerotic plaque of patients, we must accept molybdenum was removed from the centre the of enzymes. It is known that xanthine oxidoreductase (XOR) is a molybdenum enzyme, which catalyses the oxidation of xanthine in the purine metabolism to uric acid. This finding suggests that the

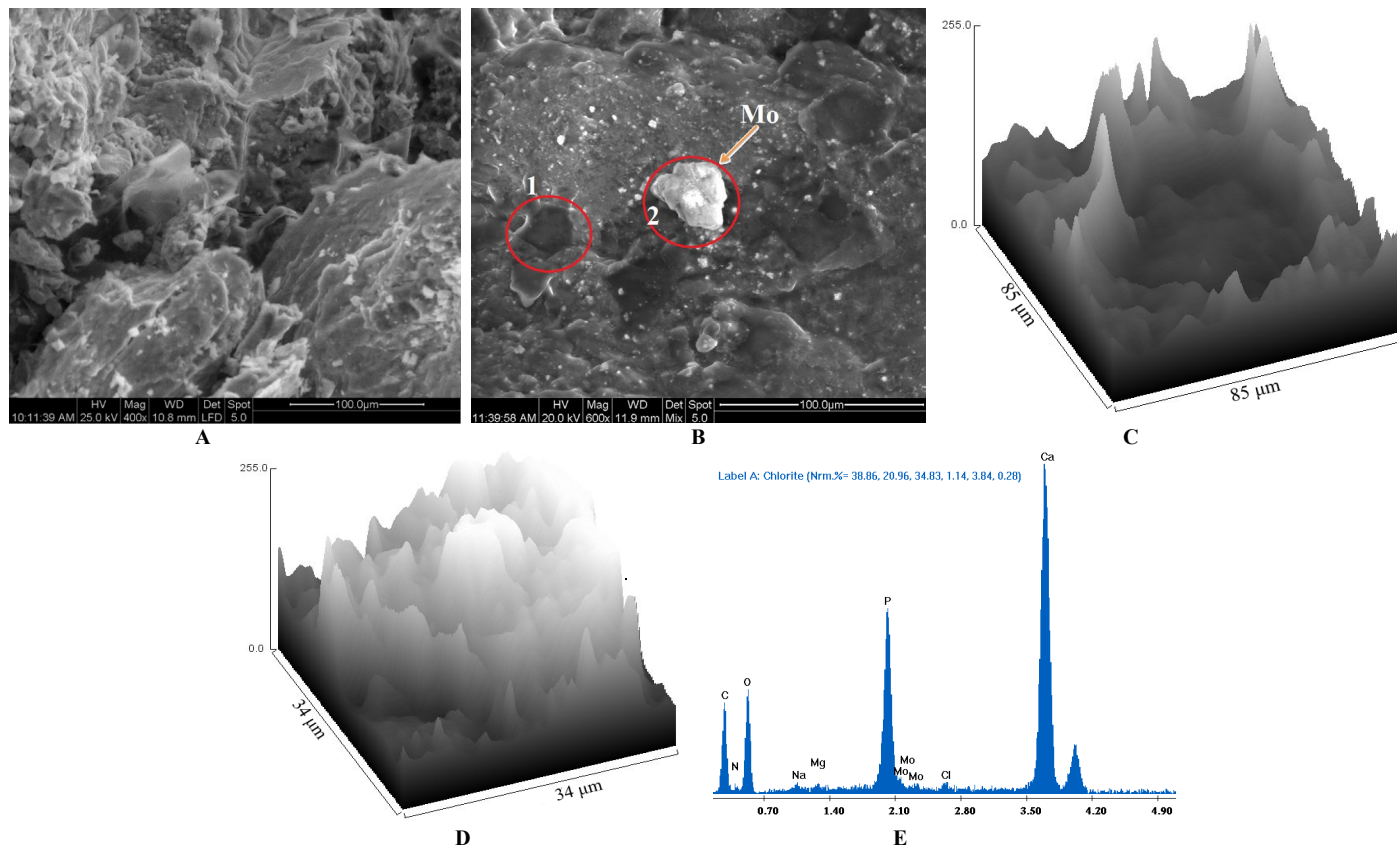


Figure 3. A) SEM illustration of carotid artery architecture of a hyperuricaemic patient. B) SEM morphology in salts rich region. C, D) ImageJ analysis of the region rich in foam cells (1) and the white spot (2), where the arrow shows the molybdenum deposit. E) SEM-EDX elementary analysis of the atheromatic components of the picture B.

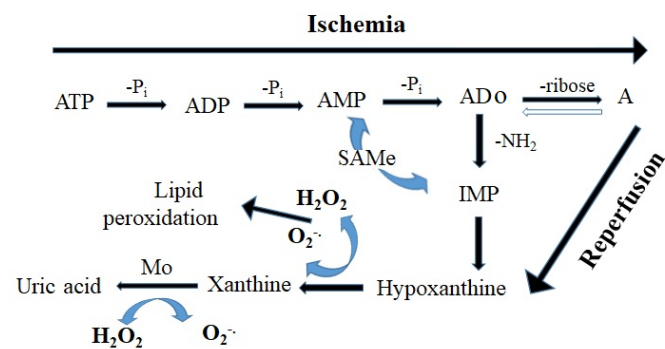


Figure 4. Schematic representation of uric acid production in the cycle ischemia-reperfusion injury. The steps of ATP dephosphorylation, hydrogen peroxide and superoxide anion free radical (O_2^-) production are shown. (ATP: Adenosine triphosphate; ADO: Adenosine; A: Adenine; P_i : PO_4^{3-} ; IMP: Inosine monophosphate; SAMe: S-adenosyl-L-methionine).

molybdenum cations of the enzymes react with superoxide anions (O_2^-) leading to molybdenum (Mo) release and that the xanthine oxidase (XOR) cannot normalize the uric acid of the patients anymore.

A cofactor deficiency affects the sulphur and xanthine metabolism, resulting in altered concentrations (high or low) of uric acid in the blood serum. Aldehyde catalases catalyse the oxidation reactions of aldehydes and various nitrogen cyclic compounds [34]. These data could explain the intensity increase of the absorption band at $1,741\text{ cm}^{-1}$ in the spectra of hyperuricaemic patients, which is assigned to aldehyde group ($-CHO$).

Figure 4 gives schematically the reactions which take place during ischemia and reperfusion.

The excess of uric acid increases the yield of peroxynitrite ions ($ONOO^-$), potent non free radical oxidant species, which are implicated in the pathophysiology of several cardiovascular diseases including autoimmune myocarditis, hypertension and heart failure. On the other hand, molybdenum, as a transition metal can react with hydrogen peroxide to produce reactive oxygen species (ROS), increasing thus lipid peroxidation. By increasing the number of ROS we are increasing the rate of atherosclerotic plaque formation. Animal studies showed that XOR, which causes oxidative stress, increased myocardial oxygen consumption and was associated with ischemic heart attack [35]. The involvement of free radical during ischemia/reperfusion is shown in figure 4.

The dephosphorylation of ATP gives phosphate groups that react with calcium cations and form calcium phosphate salts, which had been detected in the FT-IR spectra. In Figure 4 it is shown that during ischemia, the reverse reaction of ADP to ATP is inhibited. It was also observed that at the end of ischemic reperfusion the depletion of ATP increases by 3-fold the production of P_i (inorganic phosphates, PO_4^{3-}) [36]. Research data indicate that ATP oxidative phosphorylation plays an important role in atherosclerotic plaque formation and aortic valve calcification [37,38].

Conclusion

FT-IR spectroscopic data in combination with SEM-EDX analysis have shown that in hyperuricaemic patients with carotid artery atherosclerosis, the molybdenum is released from the active centre of molybdenoenzymes inhibiting the oxidation of hypoxanthine to xanthine, increasing the yield of uric acid, hydrogen peroxide and reactive oxygen species. The appearance of the infrared bands at

$1,741\text{ cm}^{-1}$ and $1,460\text{ cm}^{-1}$ which are related to the peroxidation of membrane lipids and phospholipids and the presence of urea molecules respectively, suggest an altered metabolic pathway. The elevated serum uric acid seems to be related to glycation products, which play crucial role in cardiovascular diseases. Moreover, FT-IR spectroscopy could be used to characterize the atheromatic plaque's components and to approach the mechanism of the plaque formation in order to design and develop new treatments.

References

- Sies H (1985) Oxidative Stress. Academic Press, London.
- Mamareli I, Pissaridi K, Dritsa V, Kotileas P, Tsiligris V, et al. (2010) Oxidative stress and atherogenesis. An FT-IR study. *In Vivo* 24: 883-888. [Crossref]
- Anastassopoulou J, Kyriakidou M, Kyriazis S, Mavrogenis A, Mamareli V, et al. (2018) Oxidative stress in aging and disease development studied by FT-IR spectroscopy. *Mech Ageing Dev* 172: 107-114. [Crossref]
- Bortels H (1930) Molybdenum as a catalyst in the biological fixation of nitrogen. *Arch Mikrobiol* 1: 333-342. [Crossref]
- Rothery R A, Workun GJ, Weiner JH (2008) The prokaryotic complex iron-sulfur molybdoenzyme family. *Biochim. Biophys Acta* 1778: 1897-1929. [Crossref]
- Oliveira-Paula GH, Pinheiro LC, Guimaraes DA, CondeTella DA, FurlanBlanco AL, et al. (2016) Tempol improves xanthine oxidoreductase-mediated vascular responses to nitrite experimental renovascular hypertension. *RedoxBiology* 8: 398-406. [Crossref]
- Ames BN, Cathcart R, Schwiers E, Hochstein P (1981) Uric acid provides an antioxidant defense in humans against oxidant- and radical-caused aging and cancer: A hypothesis. *Proc Natl Acad Sci U S A* 78: 6858-6862. [Crossref]
- Tavil Y, Kaya M, Oktar S, Sen N, Okyay K, et al. (2008) Uric acid level and its association with carotid intima-media thickness in patients with hypertension. *Atherosclerosis* 197: 159-163. [Crossref]
- Kelley EE (2015) A New Paradigm for XOR-Catalyzed Reactive Species Generation in the Endothelium. *Pharmacol Rep* 67: 669-674. [Crossref]
- Anastassopoulou J, Kyriakidou M, Malesiou E, Rallis M, Theophanides T (2019) Infrared and Raman spectroscopic studies of skin molecular disorders and cancer. *In Vivo* 33: 567-572. [Crossref]
- Mamareli V, Tanis O, Kyriakidou M, Mamareli I, Anastassopoulou J, et al. (2018) Oxidative damage of carotid arteries in diabetic patients. *Biomed J Scien Tech Res*, 3: 3267-3272.
- Kyriakidou M, Anastassopoulou J, Tsakiris A, Kouli M, Theophanides T (2017) FT-IR spectroscopic study in early diagnosis of skin cancer. *In Vivo* 31: 1131-1137. [Crossref]
- Megaloiikonos P, Panagopoulos GN, Bami M, Igoumenou VG, Dimopoulos L, et al. (2018) Harvesting, Isolation and Differentiation of Rat Adipose-Derived Stem Cells. *Curr Pharm Biotechnol* 19: 19-29.
- Theophanides T (2012) Infrared Spectroscopy-Life and Biomedical Sciences. Idem, Infrared Spectroscopy, Material Science, Engineering and Technology. InTechOpen.
- Theophanides T (2015) Infrared Spectroscopy-Anharmonicity of Biomolecules, Crosslinking of Biopolymers, Food Quality and Medical Applications. InTechOpen.
- Anastassopoulou J, Kyriakidou M, Kyriazis S, Dritsa V, Kormas T (2014) Protein folding and cancer. *Anticancer Res* 34: 5806-5709.
- Balan V, Michai CT, Cojocary FD, Uritu CM, Dodi G, et al. (2019) Vibrational spectroscopy fingerprint in medicine from molecular to clinical practice. *Materials* 12: 2884.
- Barth A, Zscherp C (2002) What vibrations tell us about proteins. *Quarterly Rev Bioph* 35: 369-430.
- Conti C, Ferraris P, Giorgini E, Rubini C, Sabbatini S, et al. (2008) FT-IR Microimaging Spectroscopy: Discrimination between healthy and neoplastic human colon tissues. *J Mol Struc* 881: 46-51.
- Mavrogenis AF, Megaloiikonos P, Panagopoulos G, Papagelopoulos PJ, Theophanides T, et al. (2015) Side effects of radiation in bone and cartilage: an FT-IR analysis. *J Long-Term Eff Med Implants* 25: 289-295. [Crossref]
- Kyriakidou M, Mavrogenis AF, Kyriazis S, Markouizou A, Theophanides T, et al. (2016) An FT-IR spectral analysis of the effects of γ -radiation on normal and cancerous cartilage. *In Vivo* 30: 599-604. [Crossref]

22. Anastassopoulou J, Boukaki E, Conti C, Ferraris P, Giorgini E, et al. (2009) Microimaging FT-IR spectroscopy on pathological breast tissues. *Vibrational Spectroscopy* 51: 270-275.
23. Dritsa V, Pissaridi K, Anastassopoulou J, Koutoulakis E, Mamarelis I, et al. (2013) Investigating the mechanism of aortic valve stenosis: the role of magnesium salts. *J Cardiothorac Surg* 8: S018. [[Crossref](#)]
24. Kotoulas C, Mamarelis I, Koutoulakis E, Kyriakidou M, Mamareli V, et al. (2017) The influence of diabetes on atherosclerosis and amyloid fibril formation of coronary arteries. A FT-IR spectroscopic study. *Hell J Atheroscler* 8: 1.
25. Theophanides T, Sandorfy C (1984) *Spectroscopy of Biological Molecules*, NATO Advanced Study Institute, D. Reidel Publishing Co., Dordrecht, pp: 15-29.
26. Salaris SC, Babbs CF (1989) Effect of oxygen concentration on the formation of malondialdehyde-like material in a model of tissue ischemia and reoxygenation. *Free Radic Biol Med* 7: 603-609. [[Crossref](#)]
27. Mamarelis I, Koutoulakis E, Kotoulas C, Dritsa V, Mamareli V, et al. (2017) The Role of Oxidative Stress on Amyloid-like Protein Formation and Aortic Valve Calcification. *Hellenic J Cardiol* 58: 148-150.
28. Oliver KV, Maréchal A, Rich PR (2016) Effects of the hydration state on the Mid-infrared spectra of urea and creatinine in relation to urine analysis. *Appl Spectrosc* 70: 983-994. [[Crossref](#)]
29. Raptis SG, Anastassopoulou J, Theophanides T (2000) The urea molecule and urea-Mg complexes. A conformational and infrared spectral studies. *Theor Chem Acc* 105: 156-164.
30. Petra M, Anastassopoulou J, Theologis T, Theophanides T (2005) Synchrotron micro-FT-IR spectroscopic evaluation of normal paediatric human bone. *J Mol Structure* 78: 101-110.
31. Brandes R, Bers DM (1997) Intracellular Ca^{2+} increase the mitochondrial NADH concentration during elevated work in intact cardiac muscle. *Circulation Res* 80: 82-87.
32. Bhandary B, Marahatta A, Kim H-R, Cha HJ (2013) An involvement of oxidative stress in endoplasmic reticulum stress and its associated diseases. *Int J Mol Sci* 14: 434-456. [[Crossref](#)]
33. Verzijl N, Degroot J, Oldehinkel E, Bank RA, Thorpe SR, et al. (2000) Age-related accumulation of Maillard reaction products in human articular cartilage collagen. *Biochem J* 350: 381-338. [[Crossref](#)]
34. Van Gennip AH, Abeling NG, Stroomer AEM, Overmars H, Bakker HD (1994) The detection of molybdenum cofactor deficiency: clinical symptomatology and urinary metabolite profile. *J Inherit Metab Dis* 17: 142-145. [[Crossref](#)]
35. Rajendra NS, Ireland S, George J, Belch JJF, Lang CC, et al. (2011) Mechanistic Insights Into the Therapeutic Use of High-Dose Allopurinol in Angina Pectoris. *J Am Coll Cardiol* 58: 820-828. [[Crossref](#)]
36. Cave AC, Ingwall JS, Friedrich J, Liao R, Saupé KW, et al. (2000) ATP synthesis during low-Flow ischemia: influence of increased glycolytic substrate. *Circulation* 101: 2090-2096. [[Crossref](#)]
37. Cote N, El Hussein D, Pépin A, Guague-Olarte S, Ducharme V, Bouchard-Cannon P, et al. (2012) ATP acts as a survival signal and prevents the mineralization of aortic valve. *J Mol Cellular Cardiol* 52: 1191-1202. [[Crossref](#)]
38. Kohlhaas M, Maack C (2013) Calcium release microdomains and mitochondria. *Cardiovasc Res* 98: 259-268. [[Crossref](#)]